Supplementary Information for

$K_5Eu(MoO_4)_4$ red phosphor for solid state lighting applications, prepared by different techniques

Svetlana M. Posokhova, Vladimir A. Morozov, Dina V. Deyneko, Boris S. Redkin, Dmitry A. Spassky, Vitali Nagirnyi, Alexei A. Belik, Joke Hadermann, Erzhena T. Pavlova, Bogdan I. Lazoryak

Table S1. EDX analysis results of $K_5Eu(MoO_4)_4$ prepared by different techniques.

Preparation	Solid-state synthesis	Sol-gel method followed by annealing at 893 K	Czochralski technique
K, at.%	50.23±3.20	48.63±3.25	47.79±1.86
Mo, at.%	39.34±2.17	41.55±2.81	42.54±2.13
Eu, at.%	10.43±1.25	9.82±1.60	9.67±0.56

Table S2. Unit cell parameters and estimated crystallite size for $K_5Eu(MoO_4)_4$ prepared by solid state synthesis (*ss*), sol-gel method followed by annealing at 893 K (*sg893*) and the Czochralski (CZ) techniques (SG $R\bar{3}m$) and reference data.

Technique	*a*, Å	*c*, Å	*V*, Å^3	Crystallite size (nm)
sg893	5.9730(1)	20.6674(7)	638.55(2)	97±14
ss	5.9758(1)	20.7091(6)	640.46(1)	94±11
CZ	5.9818(3)	20.699(1)	641.42(6)	
PDF-2, №45–0340	5.980	20.74	642.53	

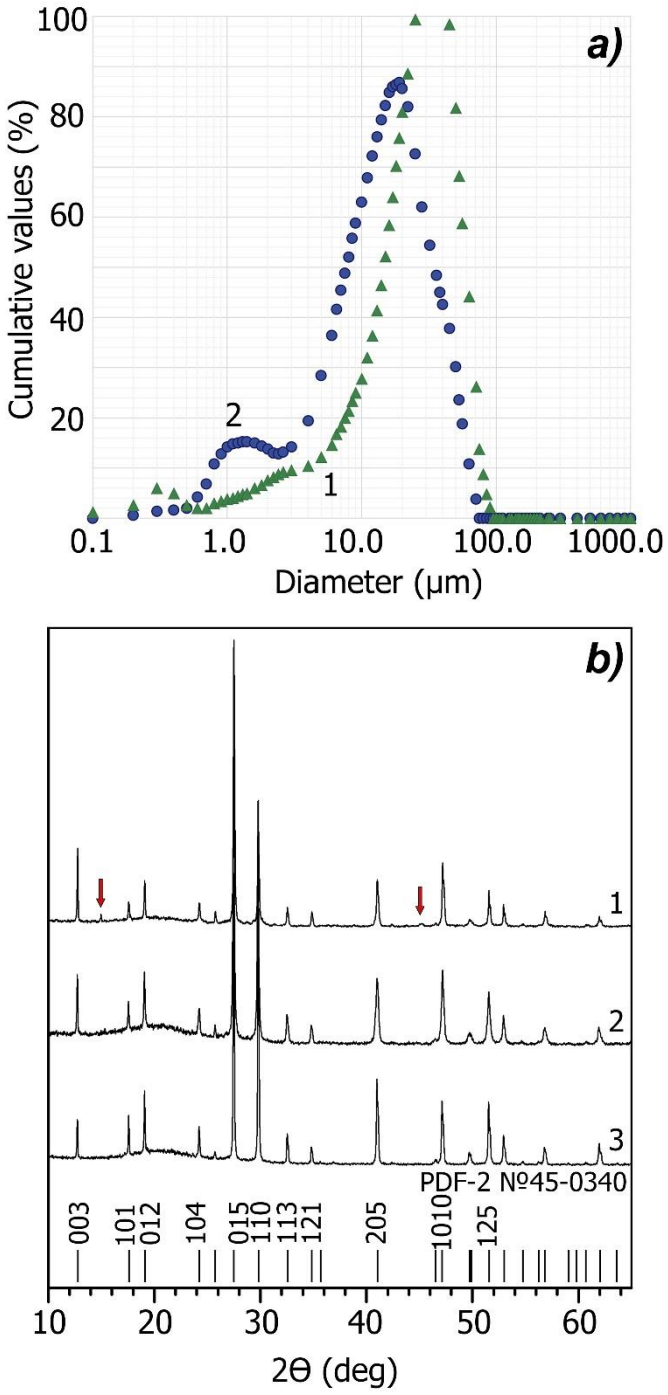

Fig. S1. Particle size distributions (*a*) and PXRD patterns (b) of $K_5Eu(MoO_4)_4$ synthesized by various methods: *sg893*-KEMO (1), ss-KEMO (2) and crushed crystal (3). Tick marks denote the peak positions of Bragg reflections for $K_5Eu(MoO_4)_4$ from ICDD Data Base (JCPDS, PDF-2, №45–0340). The *hkl* indexes for strong reflections are listed. Low intensities reflections of $K_2Mo_2O_7$ phase (PDF#2 Card no. 36-0347) in the PXRD pattern of *sg893*-KEMO are shown by red arrows.

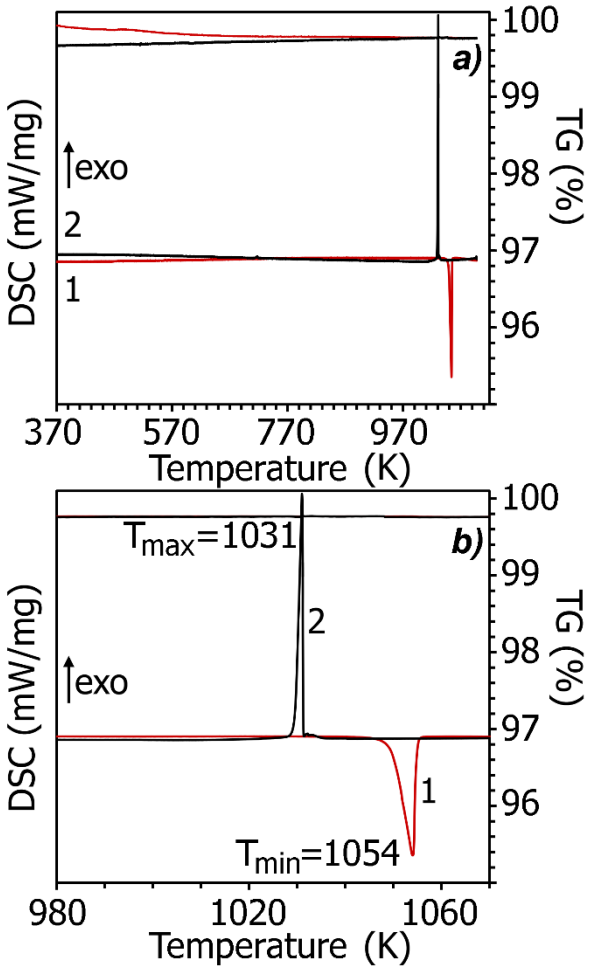

Fig. S2. Fragments of DSC and TG curves for ss-KEMO sample in the temperature ranges of 370-1120 K (*a*) and 980-1070 K (*b*) in heating (1) and cooling (2) cycle, successively.

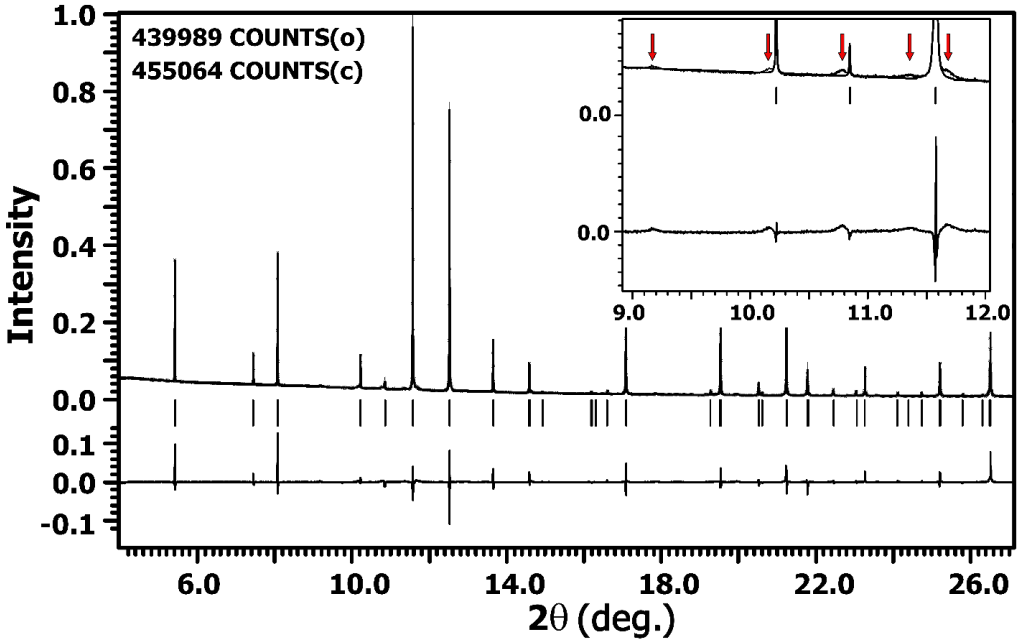

Figure S3. Fragments of the experimental, calculated and difference synchrotron XPD patterns for $K_5Eu(MoO_4)_4$ structure in the $R\bar{3}m$ model. Tick marks denote the peak positions of possible Bragg reflections. Inset shows the one of the parts of the profile with extra broad reflections shown by red arrows.

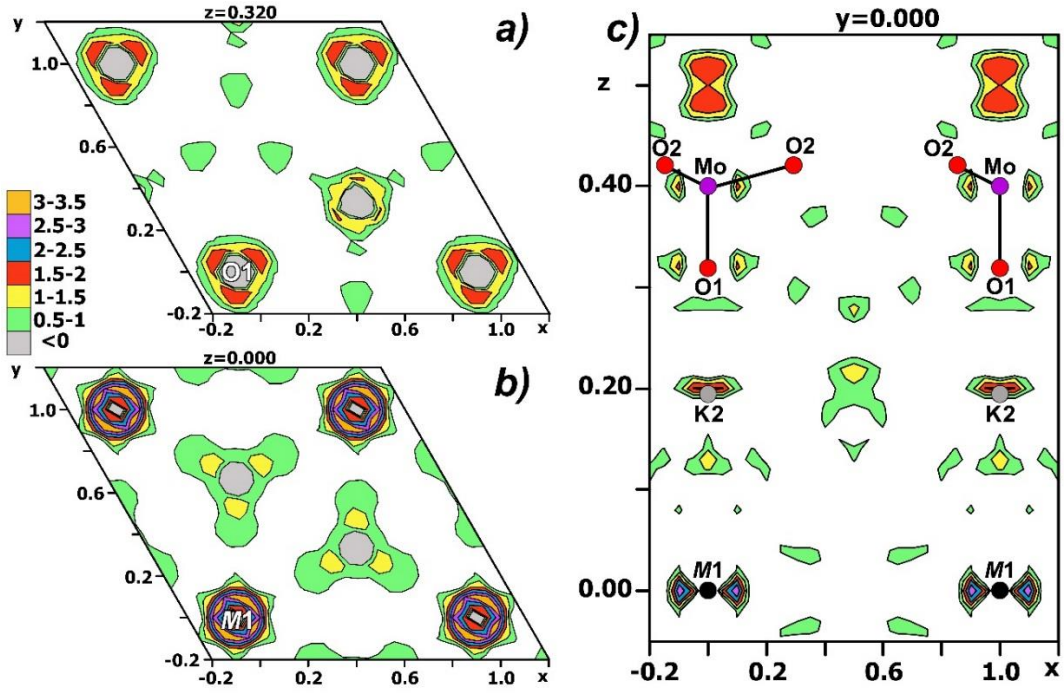

Figure S4. [ρ_{dif}: (x; y; z)] residual electron density maps for $K_5Eu(MoO_4)_4$ structure after the refinement in the $R\bar{3}m$ model in the (001) plane (*a*, *b*) through O1 (*a*) and *M*1 (*b*) atoms and in the (010) plane (*c*). Lines correspond to positive values of the electron density with 0.5 $e\times Å^{-3}$ steps, respectively. The color scale of the residual electron density is shown.

Annex 1. $R\bar{3}m$ models tested during the Rietveld refinement of $K_5Eu(MoO_4)_4$ structure using the SXPD data:

i) the original model $R\bar{3}m$: the atomic coordinates of the $K_2Pb(SO_4)_2$ structure [28-29]. In $K_2Pb(SO_4)_2$, cations occupy two crystallographic positions *M*1 (Pb) and *M*2 (K). In KEMO, potassium cations occupy the *M*2 position of the palmierite-type structure, while the *M*1 positions are statistically occupied by K^+ and Eu^{3+} (*M*1 = $0.5K^+$+$0.5Eu^{3+}$). The anion positions are fully occupied by the MoO_4^{2-} tetrahedra.

After the refinement of KEMO structure in the $R\bar{3}m$ model, the isotropic atomic displacement parameters for oxygen atoms O1 (site symmetry 6*c*) and O2 (site symmetry 18*m*) were $U_{iso.}$ = 0.1800(6) and $U_{iso.}$ = 0.062(2), respectively (Table S3). Fig. S5 shows the [ρ_{dif}: (*x*,*y*,*z*)] residual electron density maps for KEMO structure after the refinement in the $R\bar{3}m$ model in the (001) plane through O1 and *M*1 atoms and in the (010) plane. Residual electron density after refinement is observed around the O1 (~2 $e\times Å^{-3}$) and *M*1 (~3.5 $e\times Å^{-3}$) positions. Moreover, residual electron density in the (010) plane is observed in the K2 (*M*2 site) position (~2.5 $e\times Å^{-3}$) and between two MoO_4^{2-} tetrahedra on the *3-fold* axis (~2 $e\times Å^{-3}$). In the palmierite-type structure, O1 oxygen atoms as well as *M*1 and *M*2 positions lie on the *3-fold* axis and the presence of residual density shows that displacement of the O1, *M*1 and K2 atoms from the *3-fold* axis is possible in contrast to the α-$K_5Yb(MoO_4)_4$ phase [45]. Earlier, a similar displacement of these atoms from the *3-fold* axis was found during the structure refinement of α-$K_5Y(MoO_4)_4$ [46] and $M_5R(MoO_4)_4$ (*M* = K, Rb; *R* = Nd, Gd, Bi) single crystals [47].

ii) the disordered model $R\bar{3}m$: the *M*1 and O1 atoms are displaced from special positions with site symmetry 3*a* (*M*1) and 6*c* (O1) to the special position ($x, \bar{x}, z$; symmetry 18*m*). The refinement is characterized by essentially lower values of structural *R*-factors, atomic displacement parameters and max/min residual density peaks (Table S3). However, the refinement of the disordered $R\bar{3}m$ model results in a strong distortion of the MoO_4^{2-} tetrahedra (O1-Mo-O2 angles in Table S3.

Table S3. Crystallographic Data for $K_5Eu(MoO_4)_4$ in different models

Space group	Original $R\bar{3}m$ model	$R\bar{3}m$ model with *M*1 and O1 disorder	primary *C*2/*m* model
Lattice parameters: *a* (Å)	5.98647(1)	5.98663(1)	10.37099(5)
b (Å)			5.98542(3)
c (Å)	20.72495(5)	20.72517(5)	7.72496(4)
β (deg.)			116.5836(5)
V (Å^3)	643.229(2)	643.249(2)	428.831(4)
Z	1.5	1.5	1
Refinement			
№ reflections (All / Obs.)	361/313	361/306	452/436
R and R_w (%) for Bragg reflections (R_{all}/R_{obs})	14.40/12.64 and 15.10/14.99	11.18/10.17 and **12.98/12.93**	**10.23/9.44** and 13.19/13.04
R_P; R_{wP} ; R_{exp}	3.62, 6.94, 1.24	3.48,6.54, 1.24	**3.31, 6.15, 1.14**
Goodness of fit (ChiQ)	5.59	5.27	5.38
Max./min. residual density (*e*×Å^{-3})	4.10 / -7.22	3.29 / -3.92	**2.97 / -2.80**
U_{iso}(O1) (Å^2)	0.1800(6)	0.032(4)	0.061(5)
U_{iso}(O2) (Å^2)	0.062(2)	0.087(2)	0.071(4)
U_{iso}(O3) (Å^2)			0.035(4)
U_{iso}(*M*1) (Å^2)	0.0676(9)	0.027(1)	0.059(1)
Mo-O1 distance (Å)	1.554(11)	1.667(9)	1.645(13)
Mo-O2 distance (Å)	1.656(4)	1.656(4)	1.691(12)
Mo-O3 distance (Å)			1.805(16)
O1-Mo-O2 angle (Å)	103.67(18)	84.2(3), 114.5(2)	84.4(4)
O2-Mo-O2 angle (Å)	114.59(19)	113.03(17)	110.0(7)

Table S4. Fractional atomic coordinates and isotropic atomic displacement parameters (U_{iso}) for $K_5Eu(MoO_4)_4$ (SG *C*2/*m*)

Atom	*x*	*y*	*z*	U_{iso}*100	*Occup.*
*M*1(0.5Eu+0.5K)	0.0213(9)	0	-0.001(2)	3.96(1)	0.5*M*1
K	0.8259(7)	0	0.4163(6)	4.62(17)	$1K^+$
Mo	0.4014(3)	0	0.1992(3)	3.43(5)	1Mo
O1	0.3721(12)	0	0.9735(16)	6.3(6)	1O
O2	-0.001(2)	0.2650(16)	0.2215(10)	7.1(4)	1O
O3	0.2974(13)	0	0.3347(18)	4.0(4)	1O

Table S5. Selected distances (Å) and angles (◦) for $K_5Eu(MoO_4)_4$ (SG *C*2/*m*)

Polyhedra	Distance	d, Å	Polyhedra	Distance	d, Å
*M*1O_8	*M*1-O1×2	3.164(5)	KO_{10}	K-O1	2.784(11)
	*M*1-O2×2	2.268(15)		K-O2×2	3.228(16)
	*M*1-O2×2	2.424(17)		K-O2×2	3.342(15)
	*M*1-O3	2.877(14)		K-O2×2	3.015(9)
	*M*1-O3	3.154(14)		K-O3×2	3.045(2)
	<*M*1-O>	2.718		K-O3	2.746(18)
*M*1-*M*1		0.449(17)		<K-O>	3.079
Mo1O_4- tetrahedron					
Mo	O1	O2	O2	O3	
O1	1.630(13)	85.8(4)	85.8(4)	138.1(6)	
O2		1.696(12)	112.1(7)	115.1(5)	
O2		112.1(7)	1.696(12)	115.1(5)	
O3				1.808(17)	
<Mo-O>	1.708				

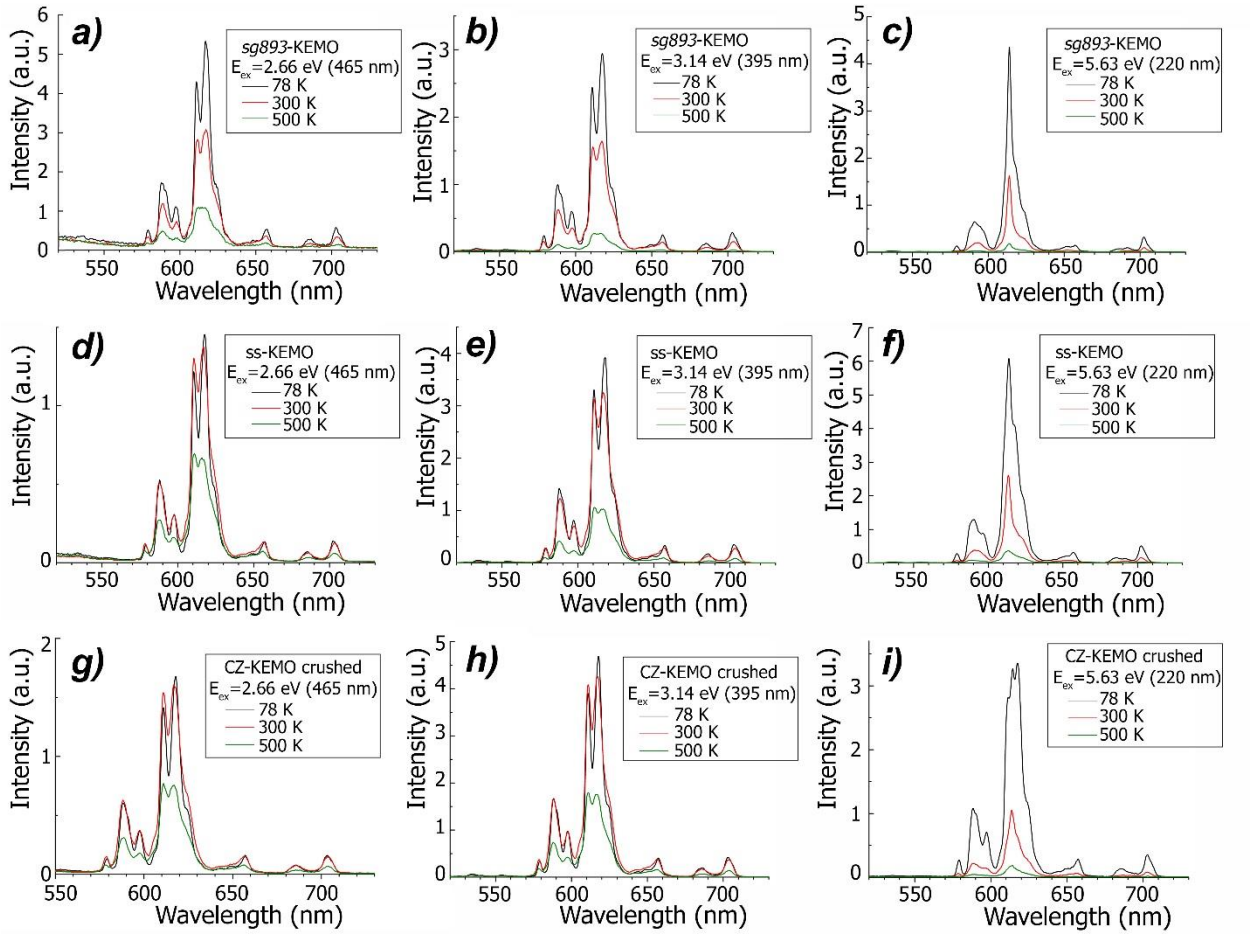

Figure S5. Photoluminescence emission spectra at temperatures 78, 300 and 500 K of *sg893*-KEMO (*a*-*c*), ss-KEMO (*d*-*f*) and crushed crystal (*g*-*i*) measured at E_{ex} = 2.66 eV (*a*, *d*, *g*); 3.14 eV (*b*, *e*, *h)* and 5.63 eV (*c*, *f*, *i*).

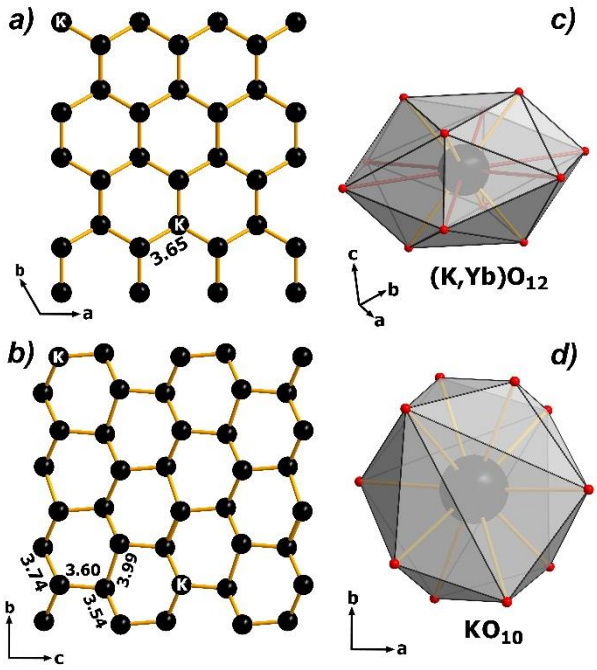

Figure S6. *M*2-layers (*a*, *b*) and K1O_n (*c*, *d*) polyhedra in the rhombohedral α-$K_5Yb(MoO_4)_4$ (*a*, *c*) and monoclinic γ-phase (*b*, *d*).

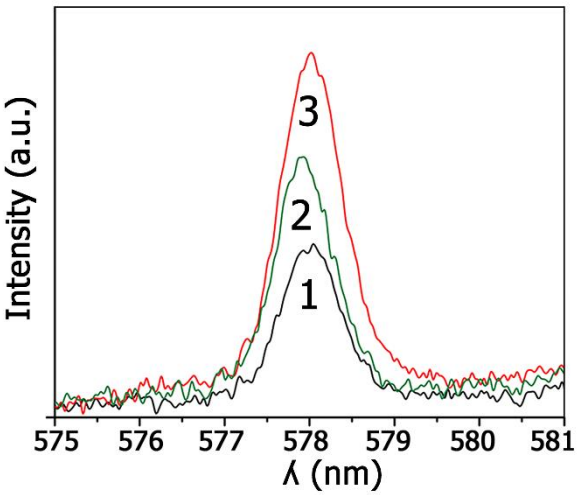

Figure S7. Photoluminescence emission spectra for the $^5D_0 \rightarrow {}^7F_0$ Eu^{3+} transition of $K_5Eu(MoO_4)_4$ at T_R: *sg893*-KEMO (1), ss-KEMO (2) and crushed crystal (3).

Table S6. Positions (λ_{max}, nm) of the $^5D_0 \rightarrow {}^7F_0$ transition, integral intensities (I_{max}, a.u.) of the $^5D_0 \rightarrow {}^7F_1$ and $^5D_0 \rightarrow {}^7F_2$ transitions, $^5D_0$-$^7F_2$/$^5D_0$-$^7F_1$ ratio (R/O), lifetimes (τ, ms) and quantum yield (QY, %) for $K_5Eu(MoO_4)_4$ prepared by solid state synthesis (*ss*), sol-gel method followed by annealing at 893 K (*sg893*) and the Czochralski (CZ) techniques. All samples are measured under the same conditions.

Technique	$^5D_0 \rightarrow {}^7F_0$, λ_{max}, nm	$^5D_0 \rightarrow {}^7F_1$, I_{max}	$^5D_0 \rightarrow {}^7F_2$, I_{max}	R/O ratio	τ, ms	QY
sg893	578.0	23738	140146	4.33	0.099, 1.282	33
ss	577.9	33583	196046	4.34	1.433	48
CZ	578.0	54866	283315	4.03	1.473	66.5